Chapter 3

Subtropical Arctic Ocean temperatures during the Paleocene-Eocene thermal maximum

The Paleocene-Eocene thermal maximum, ~55 million years ago, was a brief period of widespread, extreme climatic warming (Kennett and Stott, 1991; Zachos et al., 2003; Tripati and Elderfield, 2005) that was associated with massive atmospheric greenhouse gas input (Dickens et al., 1995). Although aspects of the resulting environmental changes are well documented at low latitudes, no data were available to quantify simultaneous changes in the Arctic region. Here we identify the Paleocene-Eocene thermal maximum in a marine sedimentary sequence obtained during the Arctic Coring Expedition (Backman et al., 2006). We show that sea surface temperatures near the North Pole increased from ~18°C to over 23 °C during this event. Such warm values imply the absence of ice and thus exclude the influence of ice-albedo feedbacks on this Arctic warming. At the same time, sea level rose while anoxic and euxinic conditions developed in the ocean's bottom waters and photic zone respectively. Increasing temperature and sea level match expectations based on paleoclimate model simulations (Shellito et al., 2003), but the absolute polar temperatures that we derive before, during and after the event are more than 10 °C warmer than model-predicted. This suggests that higher-than-modern greenhouse gas concentrations must have operated in conjunction with other feedback mechanisms – perhaps polar stratospheric clouds (Sloan and Pollard, 1998) or hurricane-induced ocean mixing (Emanuel et al., 2004) – to amplify early Paleogene polar temperatures.

Stable carbon isotope ($\delta^{13}C$) records of carbonate and organic carbon from numerous sites show a prominent negative carbon isotope excursion (CIE) across the PETM (Kennett and Stott, 1991; Koch et al., 1992). The CIE is expressed as a >2.5‰ drop in $\delta^{13}C$, which signifies an input of at least 1.5 x 10^{18}g of ^{13}C-depleted carbon, somewhat analogous in magnitude and composition to current and expected fossil fuel emissions. The PETM captures ~200kyr (Röhl et al., 2000) and is associated with profound environmental changes that are well-documented at low- to mid- latitudes (<60°), including a 4-8°C temperature rise of surface and deep ocean waters (Kennett and Stott, 1991; Zachos et al., 2003; Tripati and Elderfield, 2005) and major terrestrial and marine biotic changes (Thomas and Shackleton, 1996; Wing, 1998; Crouch et al., 2001). Terrestrial mammal turnovers are consistent with mass migrations across Arctic regions resulting from high latitude warming (Bowen et al., 2002), but no Arctic data have existed to evaluate this hypothesis.

Integrated Ocean Drilling Program Expedition 302 (or the Arctic Coring Expedition), recently recovered a Paleogene marine sedimentary record from Hole 4A (~87°52.00'N; 136°10.64'E; 1288 m water depth), on the Lomonosov Ridge in the central Arctic Ocean (Backman et al., 2006). This ridge represents a fragment of continental crust that rifted from the Eurasian shelf margin at high latitudes (>85°; Fig. 1) during the latest Paleocene and subsided to present depths after the Paleocene. Upper Paleocene and lower Eocene sediments between approximately 406 and 263 meters composite depth below seafloor (mcd) at Hole 4A consist of organic-rich (~2% total organic carbon (TOC) by mass on average) siliciclastic claystone (Backman et al., 2006). Shipboard observations showed that this interval is barren of calcareous and siliceous microfossils but yields rich assemblages of palynomorphs, notably organic-walled dinoflagellate cysts (dinocysts) and terrestrial pollen and spores (Backman et al., 2006).

The PETM was identified from the top of Core 32X to within Core 29X (~387 - 378.5 mcd) by the occurrence of the dinocyst species *Apectodinium augustum*, which is diagnostic of the PETM (Bujak and Brinkhuis, 1998) (Fig. 2; Appendix Fig. 4.1a). The lower bound is somewhat problematic, though, because the upper 50 cm of Core 32X has been disturbed by drilling and various proxies suggest that the sediment from this interval represents a mixture of latest Paleocene and PETM material (Pagani et al., 2006). Moreover, only 55 cm of section was recovered of the critical Core 31X, which has an uncertain stratigraphic position relative to Cores 30X and 32X (see error bars in Fig. 2 and Appendix 4). Stable carbon isotopes of bulk organic carbon ($\delta^{13}C_{TOC}$) show a prominent ~6‰ drop between the top of Core 32X (388 mcd) and 31X (~386 mcd), apart from one value from the disturbed zone, followed by a gradual recovery through Cores 30X and 29X to ~378.5 mcd (Fig. 2). The $\delta^{13}C_{TOC}$ pattern is generally reproduced in the carbon isotope record of the C_{27} and C_{29} *n*-alkanes, which are biomarkers derived from the leaf waxes of terrestrial higher plants (Pagani et al., 2006).

Figure 1. Location of IODP Hole 302-4A within the paleogeographic reconstruction of the Arctic Basin at late Paleocene – early Eocene times; modified from Brinkhuis et al. (2006).

Despite the core gaps, the magnitude and shape of the $\delta^{13}C_{TOC}$ excursion resembles other shallow marine PETM sections, such as Doel in Belgium (Steurbaut et al., 2003), confidently correlating this interval to the Paleocene-Eocene boundary event.

Prior to the PETM, *Apectodinium* was a subtropical dinoflagellate restricted to low latitudes (Bujak and Brinkhuis, 1998; Crouch et al., 2001). Thus, the sudden influx of *Apectodinium* spp. dinocysts across the PETM at Hole 4A (Fig. 2) suggests a substantial rise in Arctic sea surface temperature (SST) to subtropical or tropical levels. Angiosperm pollen becomes more abundant at the expense of spores and gymnosperm pollen (Fig. 2), suggesting an expanded growing season. The lack of calcareous microfossils prohibits the use of the common techniques for quantifying past SSTs. Instead, we employed the newly developed paleothermometer TEX_{86}' (see Appendix 4), which is based on the distribution

of crenarchaeotal membrane lipids (Schouten et al., 2002). This distribution is independent of surface water parameters such as nutrient availability or salinity (Schouten et al., 2002; Wuchter et al., 2004), and shows a highly significant linear correlation with present-day mean annual SST in the range of 10 to 28°C (Appendix Fig. 4.2b). Because the export of crenarchaeotal lipids to the sea floor predominantly occurs during the season with highest phytoplankton productivity, which in the Arctic Ocean is summer, our TEX_{86}' record is likely skewed towards summer temperatures (see also Appendix 4). Arctic SSTs rose from ~18°C in the latest Paleocene, to over 23°C during the PETM, and subsequently decreased to ~17°C by the end of the event (Fig. 2). Latest Paleocene and early Eocene background SSTs are generally consistent with the few other proxy data estimates from Arctic locations with late Cretaceous and early Paleogene strata (Markwick, 1998; Tripati et al., 2001; Jenkyns et al., 2004). The significantly lower terrestrial temperature estimates from Ellesmere Island at 73°N paleolatitude (Fricke and Wing, 2004) are derived from upper lower Eocene strata and similar to TEX_{86} derived SSTs in the Arctic Ocean for that time period (Brinkhuis et al., 2006), and are thus not in disagreement with our data. Maximum SSTs coincide with minimum $\delta^{13}C$ values during the PETM, while the cooling trend mirrors the recovery pattern in $\delta^{13}C$ and a decrease of angiosperm pollen.

Several lines of evidence (Fig. 2) suggest that the location of Hole 4A was proximal to the coast and strongly influenced by fluvial inputs in the latest Paleocene. For example, palynomorph assemblages from upper Paleocene strata are dominated by terrestrial spores and pollen (~90%). Those samples with sufficient dinocysts yield abundant *Senegalinium* spp. and *Cerodinium* spp. (Appendix Fig. 4.1), which likely come from dinoflagellates that tolerated low surface water salinities (Brinkhuis et al., 2006) and required nutrient-rich conditions (Appendix 1). Sediments from this interval also contain abundant amorphous organic matter, presumably of terrestrial origin. Moreover, values of the Branched and Isoprenoid Tetraether (BIT) index - a measure for the amount of river-derived terrestrial organic matter relative to marine organic matter (Hopmans et al., 2004) - are relatively high. In contrast to uppermost Paleocene sediments, palynomorph assemblages from the PETM interval are characterised by abundant dinocysts (60%) and substantially lower BIT indices (Fig. 2), indicating a relative decrease of riverine-derived organic carbon. Also the increase in the Rock Eval hydrogen index suggests a relative increase in aquatic versus terrestrial organic matter (Appendix Fig. 4.3a). We attribute the enhanced influence of marine conditions during the PETM to a sea level rise, an interpretation consistent with evidence from other neritic locations (Speijer and Morsi, 2002; Chapter 6). The gradual return to more terrestrial influence later in the event likely results from subsequent regression. Despite the transgression, low salinity tolerant dinocysts remain dominant (Fig. 2) showing that brackish surface waters persisted during the PETM. If the earliest Paleogene greenhouse world was continental ice-free, a mechanism

for the sea level rise may comprise the ~5 m thermal expansion of seawater expected from a 5-8°C (Kennett and Stott, 1991; Tripati and Elderfield, 2005) increase in deep ocean temperatures.

The occurrence of laminated sediments from the onset of the PETM (although hardly visible in Core 31X due to its disturbed state) up to 382.5 mcd, and the absence of benthic foraminiferal linings (Appendix Fig. 4.3) suggest that bottom waters became anoxic during the PETM. Within the laminated interval, derivatives of the characteristic pigment isorenieratene are recorded in concentrations up to 2 $\mu g. g^{-1}$ sediment, while they are below detection limit outside of this interval (Fig. 2; Appendix Fig. 4.3). These compounds are derived from the brown strain of photosynthetic green sulphur bacteria, which requires euxinic (anoxic and sulphidic) conditions to thrive (Sinninghe Damsté et al., 1993). Accordingly, at the PETM photic zone euxinia developed at the drill site coincident with bottom water anoxia, which gradually disappeared during the recovery of SST and $\delta^{13}C$ excursion (Fig. 2). We can exclude selective preservation as a mechanism to explain the marked changes in organic biomarkers and palynomorph assemblages that occur in coincidence with water column anoxia. First, the preservation of organic matter is also excellent outside the laminated interval (>2% TOC on average; Appendix Fig. 4.3) and second, most of our proxies compare the relative abundance of structurally similar organic compounds that are equally susceptible to oxidation (see Appendix 4).

The euxinic conditions were potentially caused by multiple factors. For example, increased fresh water input, greater nutrient load and warmer temperatures would all conspire to reduce dissolved O_2 in the water column. However, given the shallow water depth of the site, an important factor was likely intense stratification due to the influence of a brackish surface water lid. Although several mechanisms could drive such stratification, given that low salinity tolerant dinocysts remain dominant despite the more distal position of the site, and the data presented in a companion paper (Pagani et al., 2006), the simplest explanation is that decreased mixing resulted from increased SSTs and enhanced fluvial runoff, with the latter also supplying extra nutrients to increase production and saturate photic zone respiration. The termination of euxinic conditions coincides with increasing surface salinities (Pagani et al., 2006) (Fig. 2) and cooling, suggesting an increase of mixing with more saline deeper waters.

Even if we assume that our TEX_{86}' temperatures represent summer values (see Appendix 4), paleoclimate models simulating the early Paleogene world with 2000 ppmv of CO_2 in the atmosphere (Shellito et al., 2003) underestimate Arctic Ocean summer SSTs by at least 15°C for the PETM and 10°C for the surrounding late Paleocene and early Eocene. It may be suggested that this discrepancy is even larger because the initial part of the PETM, and potentially also the strata formed under maximum temperatures, were possibly not recovered

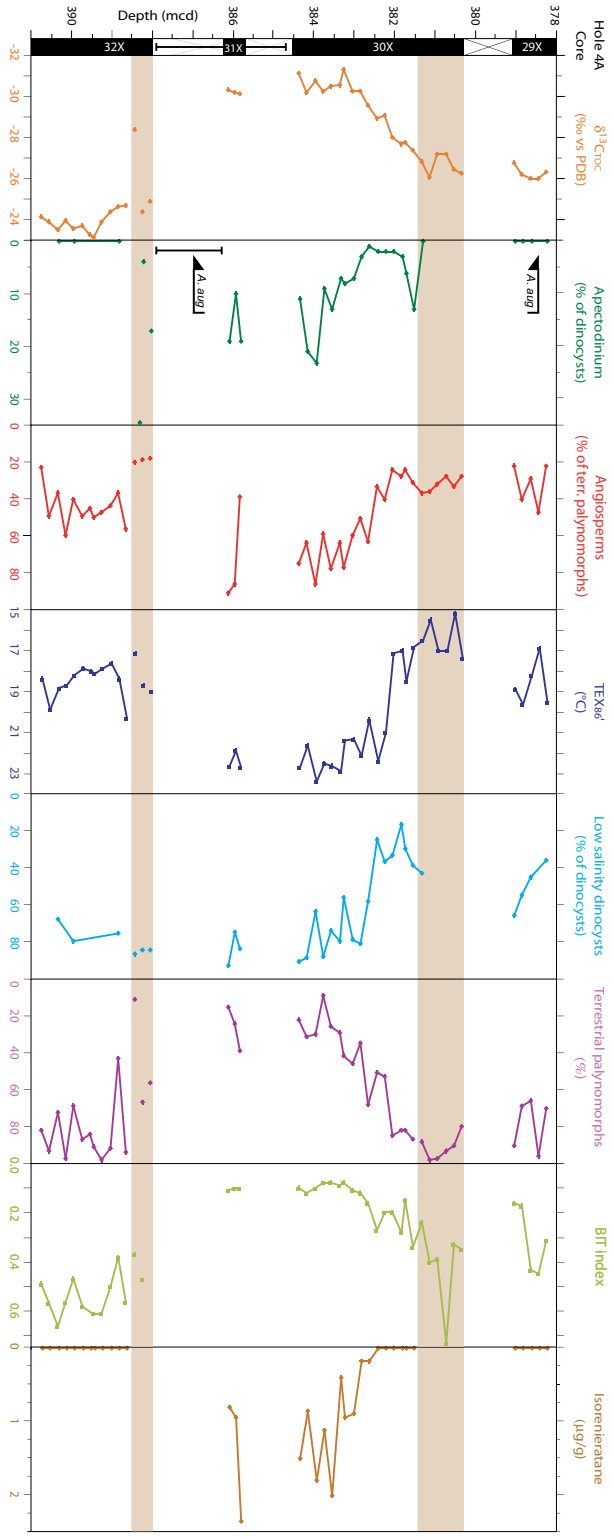

Figure 2. Core recovery and palynological and geochemical results across the PETM of IODP Hole 302-4A. Core 31X was plotted 100 cm lower relative to mcd (Backman et al., 2006) for illustration purposes. Error bars connected to Core 31X in the recovery column indicate the uncertainty of its stratigraphic position (see Appendix 4). Low salinity tolerant dinocysts comprise *Senegalinium* spp., *Cerodinium* spp., and *Polysphaeridium* spp., while *Membranosphaera* spp., *Spiniferites ramosus* complex, and *Areoligera-Glaphyrocysta* cpx. represent the typical normal marine species (Appendix 1; Appendix Fig. 4.1). Orange bars indicate intervals affected by drilling disturbance. Arrows and *A.aug* indicate first and last occurrence of dinocyst *Apectodinium augustum*.

(Fig. 2). On the other hand, the magnitude of the CIE is comparable to previous studies and peak PETM temperatures lagged the onset of the CIE by ~40kyr (Zachos et al., 2003), indicating that optimum Arctic SSTs are likely covered in our record. The models consistently predict pole-to-equator temperature gradients of ~30°C (Huber et al., 2003). Such gradients represent significant overestimates because they would imply unrealistically warm tropical SSTs considering our polar temperatures. The high polar temperatures and reduced pole-to-equator temperature gradients cannot be explained by invoking even greater greenhouse gas concentrations because this would elevate tropical SSTs, which in existing model predictions already match or exceed those determined from proxy records at low-latitude locations (Shellito et al., 2003). Also ocean heat transport is unlikely the cause because this requires a three-fold increase, which cannot be simulated in the current generation of fully coupled ocean-atmosphere climate models (Huber et al., 2003). Similarly, atmospheric general circulation models do not support strong enough positive feedbacks in atmospheric heat transport (Caballero and Langen, 2005). Consequently, we surmise that physical processes that are not yet incorporated in the models operated in conjunction with high greenhouse gas concentrations to enhance polar warmth and reduce the pole-to-equator temperature gradient during the late Paleocene to early Eocene. These processes potentially include high latitude warming and tropical cooling through the enhancement of polar stratospheric clouds (Sloan and Pollard, 1998), and hurricane-induced ocean mixing (Emanuel et al., 2004), respectively.

With latest Paleocene SSTs of 18°C it is not likely that ice was present in the Arctic. This implies that the PETM at Hole 4A allows for a unique examination of the Arctic environment and the nature of polar amplification during a time of massive greenhouse gas emissions and extreme global warming in the absence of ice-albedo feedbacks. Interestingly, polar amplification of temperature rise at the PETM appears to have been minor (Fig. 2) (Kennett and Stott, 1991; Zachos et al., 2003; Tripati and Elderfield, 2005), suggesting that the strengthening of the mechanism that caused above early Paleogene polar temperature amplification was small at the PETM. Our extremely warm polar temperatures indicate that, despite much recent progress, feedbacks responsible for early Paleogene mid- to high-latitude warmth remain poorly understood and unimplemented in existing climate models.

Methods

Palynology

Sediments were oven-dried at 60°C. To ~2 g of sediment, a known amount of Lycopodium spores were added, after which the sample was treated with 30% HCl and twice with 30% HF for carbonate and silicate removal, respectively.

After sieving over a 15-µm nylon mesh sieve, residues were analysed at 500x magnification to a minimum of 200 dinocysts. Absolute quantitative numbers were calculated using the relative number of Lycopodium.

Organic geochemistry

Powdered and freeze-dried sediments were analysed for %TOC and $\delta^{13}C_{TOC}$ with a Fison NA 1500 CNS analyser, connected to a Finnigan Delta Plus mass spectrometer. Analytical precision and accuracy were determined by replicate analyses and by comparison with international and in-house standards, and were better than 0.1% and 0.1‰ for %TOC and $\delta^{13}C_{TOC}$, respectively.

Powdered and freeze-dried sediments (1–3 g dry mass) were extracted with dichloromethane (DCM)/methanol (2:1) by using the Dionex accelerated solvent extraction technique. The extracts were separated by Al_2O_3 column chromatography using hexane/DCM (9:1) and DCM/methanol (1:1) to yield the apolar and polar fractions, respectively. The apolar fractions were analysed for isorenieratene derivatives by gas chromatography and gas chromatography/mass spectrometry, while the polar fractions were analysed for tetraether lipids and used to calculate TEX_{86}' (see Appendix 4; reproducibility = ~1°C) and BIT (see Hopmans et al., 2004, for method description) indices.